DOI: 10.1002/ejic.200800400

Ferromagnetism in Cu^{II}_4 and Co^{II}_4 Complexes Derived from Metal-Assisted Solvolysis of Di-2,6-(2-pyridylcarbonyl)pyridine: Syntheses, Structures, and Magnetic Properties

Athanassios K. Boudalis,*[a] Catherine P. Raptopoulou,[a] Vassilis Psycharis,[a] Belén Abarca,[b] and Rafael Ballesteros[b]

Keywords: Cluster compounds / Copper / Cobalt / Magnetic properties / Metal-assisted solvolysis

Metal-assisted solvolysis of di-2,6-(2-pyridylcarbonyl)pyridine (pyCOpyCOpy, dpcp) by $M(O_2CMe)_2{\cdot}xH_2O$ (M^{II} = Cu^{II}, Co^{II}) led to complex $[Cu_4\{pyC(O)_2pyC(O)(OEt)py\}(O_2CMe)_5(EtOH)_2]$ (**1**), when the reaction was carried out in EtOH, and to complex $[Co_4\{pyC(O)(OMe)pyC(O)(OMe)py\}_2(O_2CMe)_2(N_3)_2]$ (**2**), when the reaction was carried out in MeOH in the presence of azide anions. Complex **1** consists of four Cu^{II} ions bridged by the hemiacetal-*gem*-diol form of the ligand, which is found in a μ_4-η^2:η^2:η^2:η^1:η^1:η^1 coordination mode. It exhibits ferromagnetic couplings among all nearest neighbors and antiferromagnetic next-nearest-neighbor interactions ($J_{12} = J_1 = 48.0\ cm^{-1}$, $J_{23} = J_2 = 20.4\ cm^{-1}$, $J_{34} = J_3 = 16.9\ cm^{-1}$, $J_{24} = J_4 = -10.0\ cm^{-1}$, $H = -2\Sigma J_i J_j$ spin Hamiltonian formalism), which stabilize an $S = 1$ ground state and an $S = 2$ state lying closely above it. Complex **2** consists of four Co^{II} ions bridged by the bis(hemiacetal) form of the ligand, which is found in a μ_3-η^2:η^2:η^1:η^1:η^1 coordination mode, and by μ_3-azido ligands. It also exhibits ferromagnetic interactions due to the μ_3–1,1,1 bridging mode of the azido ligands, which is known to promote ferromagnetic interactions.

Introduction

The coordination chemistry of di-2-pyridyl ketone, (py_2CO, dpk) has long been used for the preparation of polynuclear transition-metal complexes, having provided a wealth of structures with a variety of metal ions.[1] The origin of this interesting chemistry is the propensity of the carbonyl function of dpk to undergo metal-assisted solvolysis (alcoholysis in alcoholic solvents or hydrolysis in non-alcoholic solvents) to yield a hemiacetal or a *gem*-diol. These forms of the ligand can undergo one or two deprotonations, respectively, thus generating anionic forms of the ligand with high coordinative versatility. On the basis of this knowledge, we surmised that the structurally relevant ligand di-2,6-(2-pyridylcarbonyl)pyridine (pyCOpyCOpy, dpcp)[2] might yield the same interesting coordination chemistry with dpk. Indeed, previous studies by Mak and co-workers corroborated this hypothesis.[3] In addition, our first such attempts in non-alcoholic media led to the icosanuclear single-molecule magnet $[Co_{20}(OH)_6(O_2CMe)_4(O_2CMe)_{18}\{pyC(O)(OH)pyCO_2py\}_4(dmf)_2]$[4] and to the pentanuclear cluster $[Cu_5(O_2CMe)_6\{pyC(O)(OH)pyC(O)(OH)py\}_2]$, in which the metal-assisted hydrolytic chemistry was observed on the carbonyl functions of dpcp (Scheme 1).[5]

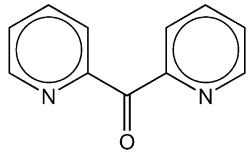

$(py)_2CO$, dpk

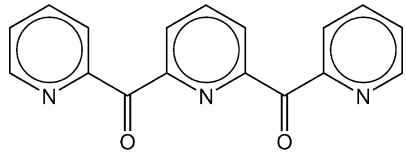

pyCOpyCOpy, dpcp

Scheme 1. The dpk and dpcp ligands.

Herein, we present the continuation of our synthetic studies employing alcoholic solvents. In particular, we report on our synthetic studies of the $M(O_2CMe)$/dpcp/ROH reaction system (M^{II} = Cu^{II}, Co^{II}; R = Me, Et) in the absence and presence of sodium azide. Structurally characterized complexes $[Cu_4\{pyC(O)_2pyC(O)(OEt)py\}(O_2CMe)_5(EtOH)_2]$ (**1**) and $[Co_4\{pyC(O)(OMe)pyC(O)(OMe)py\}_2(O_2CMe)_2(N_3)_2]$ (**2**) are studied with respect to their magnetic properties and found to exhibit ferromagnetic interactions. The origins of this ferromagnetism are discussed.

[a] Institute of Materials Science, NCSR "Demokritos", 15310 Aghia Paraskevi Attikis, Greece
Fax: +30-210-6503365
E-mail: tbou@ims.demokritos.gr
[b] Departamento de Química Orgánica, Faculdad de Farmacia, Universidad de Valencia, Avda. Vicente Andrés Estellés s/n, 46100 Burjassot (Valencia), Spain
Supporting information for this article is available on the WWW under http://www.eurjic.org or from the author.

Results and Discussion

Syntheses

In our synthetic studies of the $M(O_2CMe)_2$/dpcp/ROH reaction system, certain parameters were kept unchanged, while others were varied. The metal to ligand ratio, M^{II}/dpcp, was kept constant at 4:1, in order to favor a high degree of metallation of the ligand and hence larger nuclearities. Furthermore, the metal salt used was always the acetate. Finally, heating was always employed, since the metal-assisted solvolysis of the carbonyl function of dpk, has been shown to require a significant amount of energy in the presence of divalent metals. The same was assumed to hold here, and given the color changes upon heating, it was proven to be the case. The parameters that were varied were the metal ion (M^{II} = Cu^{II} or Co^{II}), the alcoholic solvent, ROH (R = Me or Et), and the presence or absence of azide anions. Our interest in azides is mainly fueled by their propensity to act as ferromagnetic couplers between 3d metal ions in their end-on bridging mode, but also because they are able to cause crystallization of cationic species as a result of their negative charge.

In the absence of azide anions, all four possible M^{II}/R combinations were tested. When M^{II} = Co^{II}, reaction in MeOH did not yield solid products even at high concentrations and layering with less polar solvents (e.g. Et_2O, 1:1 Et_2O/*n*-hexane), while reaction in EtOH led to immediate precipitation of powders. When M^{II} = Cu^{II}, reaction in MeOH similarly did not yield any solid products, but reaction in EtOH, and subsequent layering (Et_2O, 1:1 Et_2O/*n*-hexane, *n*-hexane), led to X-ray quality blue crystals of **1**. The reaction can be summarized by Equation (1).

$$2[Cu_2(OCMe)_4(H_2O)_2] + pyCOpyCOpy + 3EtOH \xrightarrow{EtOH} \underset{\mathbf{1}}{[Cu_4\{pyC(O)_2pyC(O)(OEt)py\}(O_2CMe)_5(EtOH)_2]} + 3MeCO_2H + 3H_2O \quad (1)$$

As a next step, we included sodium azide in the reaction mixture. In this case, when M^{II} = Co^{II} and the reaction was carried out in MeOH, complex **2** precipitated as X-ray quality pink crystals. The reaction can be summarized by Equation (2).

$$4Co(O_2CMe)_2 \cdot 4H_2O + 2pyCOpyCOpy + 2NaN_3 + 4MeOH \xrightarrow{MeOH} \underset{\mathbf{2}}{[Co_4\{pyC(O)(OMe)pyC(O)(OMe)py\}_2(O_2CMe)_2(N_3)_2]} + 4MeCO_2H + 2MeCO_2Na + 16H_2O \quad (2)$$

When, on the other hand, the reaction was carried out in EtOH, the powder that formed (see previous paragraph) did not dissolve, but instead larger quantities of it precipitated.

When M^{II} = Cu^{II}, the reaction in MeOH led to powders when the mixture was layered by nonpolar solvents, while the reaction in EtOH led directly to dark green powders.

It is noteworthy that in complex **1**, dpcp yields its asymmetrically solvolyzed hemiacetal-*gem*-diol form, while in complex **2** it yields its symmetrically alcoholyzed bis(hemiacetal) form. The reasons for this difference are currently unknown. We may assume that this may be due to the difference of the alcohol used, or the metal ions of the complex. However, without more structural data from new complexes this question may not be conclusively answered.

Description of Structures

Complex **1** crystallizes in the monoclinic *P*2/*n* space group; selected bond lengths and angles are presented in Table S1. It consists of four independent Cu atoms in a virtually linear arrangement (Figure 1). Cu1 is hexacoordinate, exhibiting a distorted octahedral coordination geometry due to Jahn–Teller elongation [Cu1–O18 2.591(1), Cu1–O13 2.443(2) Å]. Cu2, Cu3, and Cu4 exhibit square-pyramidal geometries (trigonality indices, τ = 0.07, 0.15, and 0.05, respectively), and atoms O13, O21, and O22 occupy the apical positions of each corresponding coordination sphere. The equatorial (for Cu1) and basal (for Cu2, Cu3, and Cu4) bond lengths for each corresponding Cu atom fall between 1.951–1.993, 1.908–1.977, 1.921–1.983, and 1.932–1.961 Å, respectively, the shortest such bond being Cu1–O11 and Cu1–O17 for Cu1, Cu2–N2 for Cu2, Cu3–O15 for Cu3, and Cu4–O19 for Cu4.

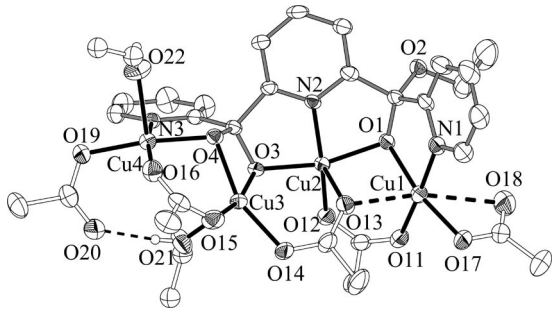

Figure 1. Partially labeled ORTEP plot of **1** at the 30% probability level. For clarity, all hydrogen atoms are omitted, except those of the hydroxy functions of the EtOH ligands.

Bridging between the metal atoms is mainly provided by the $\{pyC(O)_2pyC(O)(OEt)py\}^{3-}$ ligand, which is found in a μ_4-η^2:η^2:η^2:η^1:η^1:η^1 coordination mode. The metal ion pairs Cu1–Cu2, Cu2–Cu3, and Cu3–Cu4 are bridged by monatomic alkoxido bridges from the alkoxy atoms O1, O3, and O4, respectively, of the ligand (Scheme 2). Additional bridging is achieved through a *syn*,*syn*,*anti* μ_3-η^1:η^2 acetate (Cu1–Cu2–Cu3) and through two *syn*,*syn* μ-η^1:η^1 acetates (Cu1–Cu2 and Cu3–Cu4).

Complex **2** crystallizes in the monoclinic *I*2/m space group with one quarter of the molecule in the asymmetric unit. Selected bond lengths and angles are presented in Table S2. The complex comprises four Co^{II} atoms in a defective double cubane topology (Figure 2). The molecule sits on an inversion center generated at the cross point of a twofold axis of symmetry passing through Co1 and a mirror plane passing through Co2, the atoms of the azido and acetate ligands, as

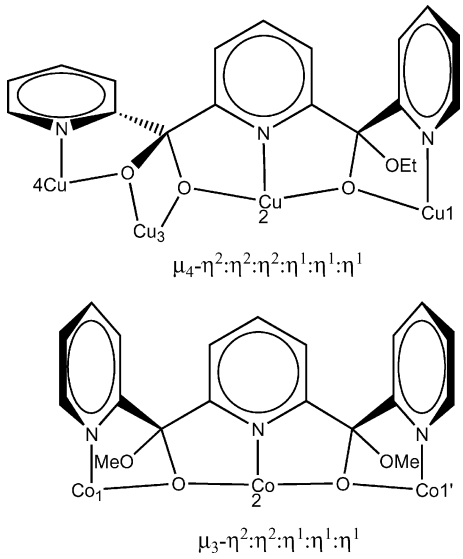

Scheme 2. Coordination modes of the ligand, as is present in **1** (top) and **2** (bottom).

well as atoms N2 and C9 of the dpcp ligand. Bridging is achieved by two dpcp ligands, which are found in their μ_3-η^2:η^2:η^1:η^1:η^1 coordination mode, and by two end-on μ_3-azido ligands.

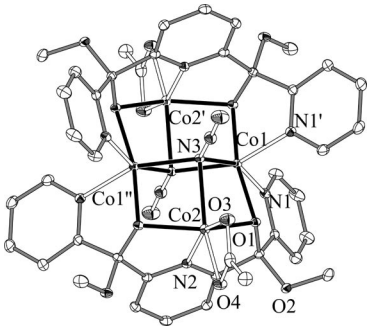

Figure 2. Partially labeled ORTEP plot of **2** at the 30% probability level. For clarity, all hydrogen atoms are omitted. Symmetry operations to generate equivalent atoms: ′ = –*x*, *y*, 1 – *z*; " = –*x*, –*y*, 1 – *z*.

Although there are a few examples of transition-metal clusters exhibiting the defective double cubane structural motif,[6] only in two such cases has the μ_3-1,1,1 azido bridging been observed: once in a complex formulated as $[Cu_4L_2(N_3)_6](ClO_4)_4$ [L^- = the monoanion of 2,2,6-bis{*N*,*N*-dimethylamino(propylamino)methyl}-4-methylphenol][7] and once in complex $[Ni_4(N_3)_8(enbzpy)_2]$ (enbzpy = [*N*,*N*-bis(pyridin-2-yl)benzylidene]ethane-1,2-diamine).[8]

Magnetic Properties of Complex 1

The $\chi_M T$ product for **1** is 2.04 $cm^3 mol^{-1} K$, which is above the value predicted for four noninteracting S = 1/2 ions (1.65 $cm^3 mol^{-1} K$, g = 2.1), suggesting ferromagnetic interactions. This is corroborated by the increase in $\chi_M T$ upon cooling, up to a maximum of 2.67 $cm^3 mol^{-1} K$ at 9 K. Further cooling leads to a sharp drop in $\chi_M T$ to 2.21 $cm^3 mol^{-1} K$ at 2 K, the origin of which will be discussed below (Figure 3).

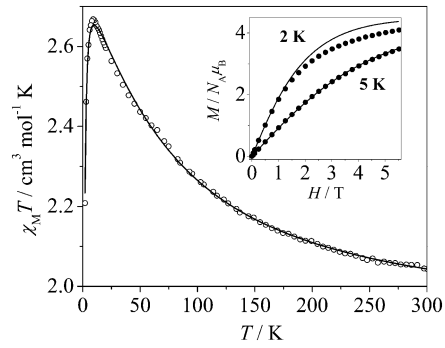

Figure 3. $\chi_M T$ vs. T data for **1**, along with the best-fit according to the model described in the text. The magnetization isotherm at 2 K (inset) agrees with a high-spin ground state.

Due to the low symmetry of **1**, which comprises four inequivalent ions with different coordination spheres and bridges between them, a model considering at least three different J constants is required for the interpretation of its magnetic susceptibility data (i.e., J_{12}, J_{23}, J_{34}). Initial attempts to fit the data by taking into account a 3J model led to very poor results. It was then considered that, because of the bridging between the metal ions, next-nearest neighbor interactions should be taken into account. Indeed, Cu1 and Cu3 are connected through a μ_3-η^1:η^2 acetate (via atoms O13–C22–O14), while Cu2 and Cu4 are connected through the $\{pyC(O)_2pyC(O)(OEt)py\}^{3-}$ ligand (via atoms O3–C12–O4). Since, however, eventual superexchange between Cu1 and Cu3 would be transmitted through atom O13, which is bonded to a nonmagnetic orbital, this exchange is expected to be negligible. Therefore, the Hamiltonian given in Equation (3) was used.

$$\hat{H} = -2[J_1\hat{S}_1\hat{S}_2 + J_2\hat{S}_2\hat{S}_3 + J_3\hat{S}_3\hat{S}_4] - 2J_4\hat{S}_2\hat{S}_4 \quad (3)$$

Fitting of the data yielded the best-fit parameters J_1 = 48.0 cm^{-1}, J_2 = 20.4 cm^{-1}, J_3 = 16.9 cm^{-1}, J_4 = –10.0 cm^{-1}, g = 2.24 ($R = 1.0 \times 10^{-5}$). This solution implies an S = 1 ground state and an S = 2 state situated only 1.2 cm^{-1} higher. This ground state is the result of the J_4 interaction, without which the ground state would be S = 2. This interaction is critical for the reproduction of the experimental data, since its elimination leads to great deviations of the calculated $\chi_M T$ vs. T curves. We are, therefore, confident of the necessity of including it in our model (Figure 4).

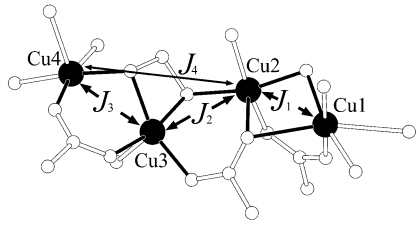

Figure 4. Spin-coupling scheme in complex **1**.

Additional verification of the employed model and the derived solution came from error-contour plots calculated for all possible combinations of J_1, J_2, J_3, and J_4. All six plots confirmed that nearest-neighbor exchange couplings should be ferromagnetic and that the Cu2–Cu4 coupling should be antiferromagnetic, in agreement with our fits.

Finally, the derived solution was further verified by conducting simulations of the *M* vs. *H* data collected at 2 and 5 K. By using the best-fit parameters, the magnetization isotherms at these two temperatures were calculated. The agreement at 5 K was perfect, while a small disagreement with the 2-K data was attributed to small zero-field-splitting effects. We propose that this behavior is analogous to that previously observed for a Cu_5 cluster.[5] A probable cause for zfs is the presence of anisotropic interactions, which, however, cannot be accounted for in the frame of the current model.

Magnetostructural Correlations

The signs and magnitudes of the *J* constants deserve some further comment. The most outstanding features of the present results are the strong ferromagnetic couplings between all Cu^{II} ions. Magnetic exchange between Cu^{II} ions is mainly propagated through their magnetic orbitals, which occupy the basal or equatorial coordination positions (in the cases of tetragonal pyramidal or octahedral coordination, respectively). Inversely, the apical or axial positions transmit negligible magnetic exchange. Empirical magnetostructural correlations by Hatfield and Hodgson[9] for the magnetic exchange within dimers in the planar $\{Cu_2(OH)_2\}^{2+}$ core have shown that below a Cu–O–Cu angle of 97.5° ferromagnetic interactions could be anticipated. Later, Kahn et al.[10] showed that for a nonplanar Cu_2O_2 core, the dihedral angle between the two CuO_2 planes is quite influential on the net magnetic coupling. In particular, it was shown that for a symmetric Cu_2O_2 core with Cu–O–Cu angles of 105.5°, a dihedral angle below 130° induces a switch to a net ferromagnetic exchange. Obviously, the case is more complicated for a Cu_2O_2 core with different Cu–O–Cu angles, or when the bridges are different, thus invoking the concept of complementarity or countercomplementarity of the magnetic orbitals.[11]

Although a full theoretical analysis of the magnetic couplings exceeds the scope of this work, we shall provide a qualitative one. In the present case, the metal cores exhibit more complicated bridging; however, we may draw some conclusions by comparing them with the above-mentioned theoretical studies. The magnetic orbitals of the Cu^{II} ions are occupied by the equatorial donor atoms in the case of Cu1 (O1/O11/O17/N1) and by the basal donor atoms in the cases of Cu2 (O1/O12/O3/N2), Cu3 (O3/O4/O15/O14), and Cu4 (O4/O16/O19/N3).

Monatomic O bridges present within these basal planes form Cu–O–Cu angles of 98.75° (Cu1–O1–Cu2), 115.59° (Cu2–O3–Cu3), and 106.22° (Cu3–O4–Cu4). Although the first such angle is acute enough to mediate a strong ferromagnetic coupling, the two others are not so acute as to justify the derived values, so additional explanation is required.

We could assume that the carboxylate bridges of the three Cu–Cu pairs exert a countercomplementarity effect, diminishing possible antiferromagnetic contributions associated with the obtuse Cu–O–Cu angles. This effect is expected to be more pronounced between the pairs Cu1–Cu2 and Cu3–Cu4, in which the carboxylate bridges occupy magnetic orbitals of the Cu^{II} atoms. In fact, bonds Cu1–O11 and Cu2–O12 are the shortest ones in each coordination sphere of the Cu1–Cu2 pair (1.951 and 1.909 Å, respectively). The same holds for the Cu3–O15 bond, which is the shortest one in the coordination sphere of Cu3 (1.921 Å), while Cu4–O16 is relatively short as well (1.961 Å).

These arguments, however, fail so far to account for the ferromagnetic coupling of the Cu2–Cu3 pair, in which the carboxylate bridge occupies a nonmagnetic orbital of Cu2. The mean equatorial and basal planes of the Cu^{II} atoms form dihedral angles, which substantially deviate from coplanarity. The dihedral angles for these planes are 122.3° (Cu1/Cu2), 110.9° (Cu2/Cu3), and 117.6° (Cu2/Cu3), leading to poor overlap of the magnetic orbitals and a consequent quenching of the antiferromagnetic component of the magnetic exchange. A similar situation was observed in a previously reported Cu^{II}_5 complex of the same ligand, in which a dihedral angle of 118.6° between two Cu^{II} ions was accompanied by ferromagnetic coupling of the two spins (J = +39.7 cm^{-1}). An acetate ligand bridging the two ions may also be responsible for this ferromagnetic value, because of its countercomplementarity effect. It may be argued that, due to the steric requirements of the ligand and the subsequent dihedral angles that arise for Cu^{II} ions bridged by its alkoxido/hydroxido functions, it may act as an efficient ferromagnetic coupler, even in the absence of azides.

As for the next-nearest-neighbor interaction J_{24}, it should be noted that the superexchange pathway provided by the ligand (O3–C12–O4) mediates magnetic exchange through the magnetic orbitals of Cu2 and Cu4, since O3 and O4 occupy basal positions of the coordination spheres of these ions. Inversely, the exchange pathway between Cu1 and Cu3 (O13–C22–O14) is expected to be much less effective, since it entails atom O14, which occupies one of the axial positions of Cu1 and does not coincide with a magnetic orbital.

Magnetic Properties of Complex 2

The $\chi_M T$ product for **2** is 11.92 $cm^3 mol^{-1} K$, significantly higher than the value predicted for four noninteracting S = 3/2 ions (7.50 $cm^3 mol^{-1} K$, g = 2). This is partly due to the orbital contributions of high-spin Co^{II} ions in octahedral environments, which are known to be important, but also due to the existence of intramolecular ferromagnetic interactions. This is corroborated by the continuous increase in $\chi_M T$ upon cooling, up to a maximum of 27.44 $cm^3 mol^{-1} K$ at 6 K. The decrease below that temperature is attributed to the combined effect of zero-field splitting and Zeeman interactions. However, due to the complications introduced by the orbital

contributions of Co^{II} ions, a quantitative treatment of the magnetic susceptibility data of **2** was not attempted. The high-spin ground state of **2** is illustrated by its magnetization isotherm at 2 K, which shows the onset of saturation above 1 T (Figure 5, inset). Although the saturation is not complete up to 5.5 T, its value is expected to be well over 10 $N_A\mu_B$, indicative of a high-spin ground state.

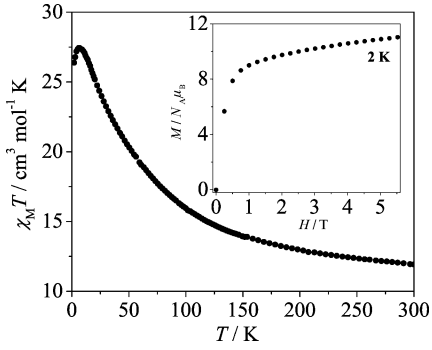

Figure 5. $\chi_M T$ vs. T data for **2**. The magnetization isotherm at 2 K (inset) agrees with a high-spin ground state.

The ferromagnetic coupling within **2** may be rationalized by the presence of two end-on μ_3-azido ligands, which form Co–N–Co angles that favor ferromagnetic couplings (Co1–N3–Co2 = Co1′′–N3–Co2 = 89.78°). The high-spin ground state of **2** prompted us to test whether slow magnetic relaxation effects are manifested at low temperatures. Experiments of ac magnetic susceptibility between 2–7 K and at frequencies between 11–8111 Hz did not yield significant out-of-phase signals, thus precluding the appearance of slow magnetic relaxation effects.

Conclusions

Dpcp is a relatively unexplored ligand, but the similarities of its coordination chemistry to that of dpk render it particularly interesting for the preparation of polynuclear transition-metal complexes. Its use in alcoholic ligands revealed that different forms of its alcoholyzed form are accessible, in our case the *gem*-diol-hemiacetal (in **1**) and the bis(hemiacetal) (in **2**) forms. Both complexes exhibit intramolecular ferromagnetic interactions, stabilizing high-spin ground states, but the origin of these interactions is different for the two complexes. In complex **1**, the main cause for the observation of ferromagnetic interactions is the poor overlap of the magnetic orbitals of the Cu^{II} ions. This is due to the geometric constrains imposed by $[pyC(O)_2pyC(O)(OEt)py]^{3-}$ to neighboring Cu^{II} ions bridged through its alkoxy oxygen atoms. A similar observation in a Cu^{II}_5 complex previously reported[5] seems to suggest that the various forms of dpcp may favor ferromagnetic interactions between Cu^{II} ions, precisely due to these geometric constrains. On the other hand, the ferromagnetism observed in **2** is the consequence of the μ_3-1,1,1 bridging mode of the azide anions, which are known to favor ferromagnetic interactions between transition-metal ions when acting as end-on bridges. These conclusions will be used for the design of new complexes of dpcp, with the aim of obtaining high-spin ground states and hopefully interesting magnetic properties.

Experimental Section

$[Cu_4\{pyC(O)_2pyC(O)(OEt)py\}(O_2CMe)_5(EtOH)_2]\cdot EtOH$ (1·EtOH): Solid dpcp (50.0 mg, 0.173 mmol) was added to a solution of $[Cu_2(O_2CMe)_4(H_2O)_2]$ (0.138 g, 0.346 mmol) in EtOH (35 mL). Upon dissolution, the color of the solution changed from blue-green to light blue, and upon heating under reflux for ca. 15 min, the color turned to blue. The solution was layered with twice its volume of Et_2O, yielding light blue needles of **1**·EtOH. The mother liquor was removed by decantation, and the crystals were repeatedly washed with Et_2O and dried in vacuo. The yield was 63 mg (≈ 37% with respect to dpcp). The dried sample was solvent-free according to analysis results. $C_{33}H_{43}Cu_4N_3O_{16}$ (991.90): calcd. C 39.96, H 4.37, N 4.22; found C 39.88, H 4.48, N 4.19. IR (KBr): $\tilde{\nu}$ = 2976 (m [$\nu(CH_3)$]), 2932 (m [$\nu(CH_2)$]), 1604 (vs. [$\nu(C{=}C) + \nu(C{=}N)$]), 1566 (vs. [$\nu_{as}(COO)$]), 1431 (vs. [$\nu_s(COO_{bridging})$]), 1406 (s [$\nu_s(COO_{monodentate})$]), 1090 (s [$\nu(C–O)_{dpcp}$]), 1049 (s [$\nu(C–O)_{EtOH}$]), 686 (m [$\pi(C–H)_{py}$]) cm^{-1}.

$[Co_4\{pyC(O)(OMe)pyC(O)(OMe)py\}_2(O_2CMe)_2(N_3)_2]\cdot 0.8H_2O$ (2·0.8H$_2$O): Solid dpcp (50.0 mg, 0.173 mmol) was added to a solution of $Co(O_2CMe)_2\cdot 4H_2O$ (0.172 g, 0.691 mmol) in MeOH (20 mL). Upon dissolution, the color of the solution changed from purple to wine-red, and upon heating under reflux for ca. 15 min the color turned to purple-red. The resulting solution was cooled to room temperature, and a solution of NaN_3 (44.0 mg, 0.691 mmol) in MeOH (20 mL) was added, causing a color change to dark red. After 3 d of being kept in a capped flask, a crystalline solid of **2**·0.8H$_2$O formed. The mother liquor was removed by decantation, and the crystals were repeatedly washed with MeOH and dried in vacuo. The yield was 58 mg (≈ 61% with respect to dpcp). The dried sample was solvent-free according to analysis results. $C_{42}H_{40}Co_4N_{12}O_{12}$ (1140.59): calcd. C 44.23, H 3.54, N 14.74; found C 44.16, H 3.60, N 14.79. IR (KBr): $\tilde{\nu}$ = 2966 (m [$\nu(CH_3)$]), 2074 (vs. [$\nu(N_3)$]), 1600 (m [$\nu(C{=}C) + \nu(C{=}N)$]), 1539 (m [$\nu_s(COO_{chelating})$]), 1443 [$\nu_s(COO_{bridging})$], 1073 (s [$\nu(C–O)_{dpcp}$]), 673 (m [$\pi(C–H)_{py}$]) cm^{-1}.

X-ray Crystallography: A blue crystal of **1** (0.08 × 0.18 × 0.33 mm) was mounted in a capillary and a pink crystal of **2** 0.10 × 0.20 × 0.30 mm was taken directly from the mother liquor and immediately cooled to –170 °C. Diffraction measurements were made with a Rigaku R-AXIS SPIDER Image Plate diffractometer by using graphite monochromated radiations of Cu-K_α for **1** and Mo-K_α for **2**. Data collection (ω-scans) and processing (cell refinement, data reduction and empirical absorption correction) were performed with the CrystalClear program package.[12] The structure was solved by direct methods by using SHELXS-97[13] and refined by full-matrix least-squares techniques on F^2 with SHELXL-97.[14] Crystal data collection and refinement parameters are presented in Table 1. Further experimental crystallographic details for **1**: $2\theta_{max}$ = 118° (complete data to $2\theta_{max}$ = 143° were collected but they were omitted during the refinement of the structure, because in high 2θ values more than half the data collected were unobserved); $(\Delta/\sigma)_{max}$ = 0.003; $(\Delta\rho)_{max}/(\Delta\rho)_{min}$ = 0.444/–0.436 e Å^{-3}. The hydrogen atoms were either located by difference maps and were refined isotropically or were introduced at calculated positions as riding on bonded atoms. All non-hydrogen atoms were refined anisotropically. Further experimental crystallographic details for **2**: $2\theta_{max}$ = 51°; $(\Delta/\sigma)_{max}$ = 0.000; $(\Delta\rho)_{max}/(\Delta\rho)_{min}$ = 1.356/–0.518 e Å^{-3}. All hydrogen atoms were

located by difference maps and were refined isotropically; no hydrogen atoms for the water solvate were included in the refinement. All non-hydrogen atoms were refined anisotropically.

Table 1. Crystal data for complexes **1** and **2**.

	1·EtOH	**2**·0.8H_2O
Formula	$C_{35}H_{49}Cu_4N_3O_{17}$	$C_{42}H_{41.6}Co_4N_{12}O_{12.8}$
FW	1037.93	1155.00
T [K]	293(2)	103(2)
Crystal system	monoclinic	monoclinic
Space group	$P2/n$	$I2/m$
a [Å]	8.0045(2)	11.272(3)
b [Å]	20.0251(5)	14.252(4)
c [Å]	28.3115(8)	14.607(5)
β [°]	91.116(2)	101.37(2)
V [Å^3]	4537.2(2)	2300.5(12)
Z	4	2
$\rho_{calcd.}$ [g cm^{-3}]	1.519	1.667
λ [Å]	1.51187	0.71073
μ [mm^{-1}]	2.711	1.495
Refl. measd./unique	25859/6374 [R_{int} = 0.0577]	6854/2176 [R_{int} = 0.0253]
Refl. obsd. [$I > 2\sigma(I)$]	5050	1907
Parameters refined	600	222
$R1$, $wR2$ (all)	0.0552/0.1281	0.0415/0.0981
$R1$, $wR2$[a] (obsd.)	0.0416/0.1127	0.0366/0.0951

[a] $R1 = \Sigma(||F_o| - |F_c||)/\Sigma(|F_c|)$; $wR2 = \{\Sigma[w(F_o^2 - F_c^2)^2]/\Sigma[w(F_o^2)^2]\}^{1/2}$, $w = 1/[\sigma^2(F_o^2) + (aP)^2 + bP]$, $P = [\max(F_o^2,0) + 2F_c^2]/3$.

CCDC-685257 (for **1**) and CCDC -685258 (for **2**) contain the supplementary crystallographic data for this paper. These data can be obtained free of charge from the Cambridge Crystallographic Data Centre via www.ccdc.cam.ac.uk/data_request/cif.

Physical Measurements: Elemental analysis for carbon, hydrogen, and nitrogen was performed on a Perkin–Elmer 2400/II automatic analyzer. Infrared spectra were recorded by using KBr pellets in the range 4000–400 cm^{-1} with a Bruker Equinox 55/S FT-IR spectrophotometer. Variable-temperature magnetic susceptibility measurements were carried out on polycrystalline samples of **1** and **2** in the 2–300 K temperature range by using a QuantumDesign MPMS SQUID susceptometer operating at 5 kG and 1 kG, respectively. Magnetization isotherms between 0 and 5.5 T were collected at 2 K. The ac susceptibility measurements on complex **2** were carried out with a QuantumDesign PPMS. Diamagnetic corrections for the complexes were estimated from Pascal's constants. The magnetic susceptibility for **1** has been computed by exact calculation of the energy levels associated with the spin Hamiltonian through diagonalization of the full matrix with a general program for axial symmetry.[15] Least-squares fittings were accomplished with an adapted version of the function-minimization program MINUIT.[16] The error-factor R is defined as $R = \Sigma \frac{(\chi_{exp.} - \chi_{calcd.})^2}{N\chi_{exp.}^2}$, where N is the number of experimental points. Simulations of the magnetization M vs. applied field H were carried out with the MAGPACK program package by using parameters derived from fits of the magnetic susceptibility.[17]

Supporting Information (see footnote on the first page of this article): Selected bond lengths and angles for complex **1** and complex **2** are presented in Table S1 and Table S2, respectively. Figures S1 and S2 contain error contour-plots for all various combinations of J_1, J_2, J_3, and J_4.

Acknowledgments

We are grateful to the Ministerio de Educación y Ciencia (Spain) (Project CTQ2006-15672-C05-03) for financial support and to the European Regional Development Fund for co-financing.

[1] a) G. S. Papaefstathiou, S. P. Perlepes, *Comments Inorg. Chem.* **2002**, *23*, 249; b) A. K. Boudalis, B. Donnadieu, V. Nastopoulos, J. M. Clemente-Juan, A. Mari, Y. Sanakis, J.-P. Tuchagues, S. P. Perlepes, *Angew. Chem. Int. Ed.* **2004**, *43*, 2266; c) A. K. Boudalis, Y. Sanakis, J. M. Clemente-Juan, B. Donnadieu, V. Nastopoulos, A. Mari, Y. Coppel, J.-P. Tuchagues, S. P. Perlepes, *Chem. Eur. J.* **2008**, *14*, 2514.

[2] B. Abarca, R. Ballesteros, M. Elmasnaouy, *Tetrahedron* **1998**, *54*, 15287.

[3] a) X.-D. Chen, T. C. W. Mak, *Inorg. Chim. Acta* **2005**, *358*, 1107; b) X.-D. Chen, M. Du, F. He, X.-M. Chen, T. C. W. Mak, *Polyhedron* **2005**, *24*, 1047; c) X.-D. Chen, T. C. W. Mak, *J. Mol. Struct.* **2005**, *748*, 183.

[4] A. K. Boudalis, C. P. Raptopoulou, B. Abarca, R. Ballesteros, M. Chadlaoui, J.-P. Tuchagues, A. Terzis, *Angew. Chem. Int. Ed.* **2006**, *45*, 432.

[5] A. K. Boudalis, C. P. Raptopoulou, V. Psycharis, Y. Sanakis, B. Abarca, R. Ballesteros, M. Chadlaoui, *Dalton Trans.* **2007**, 3582.

[6] See references in: A. Escuer, G. Aromí, *Eur. J. Inorg. Chem.* **2006**, 4721.

[7] J. Lorösch, H. Paulus, W. Haase, *Inorg. Chim. Acta* **1985**, *106*,101.

[8] T. K. Karmakar, S. K. Chandra, J. Ribas, G. Mostafa, T. H. Lu, B. K. Ghosh, *Chem. Commun.* **2002**, 2364.

[9] V. H. Crawford, H. W. Richardson, J. R. Wasson, D. J. Hodgson, W. E. Hatfield, *Inorg. Chem.* **1976**, *15*, 2107.

[10] M. F. Charlot, S. Jeannin, O. Kahn, J. Lucrece-Abaul, J. Martin-Frere, *Inorg. Chem.* **1979**, *18*, 1675.

[11] O. Kahn, *Molecular Magnetism*, Wiley, New York, **1993**, pp. 164–167.

[12] Rigaku/MSC (**2005**). *CrystalClear*. Rigaku/MSC Inc., The Woodlands, Texas, USA.

[13] Sheldrick, G. M., *SHELXS-97: Structure Solving Program*, University of Göttingen, Germany, **1997**.

[14] Sheldrick, G. M., *SHELXL-97: Crystal Structure Refinement Program*, University of Göttingen, Germany, **1997**.

[15] J.-M. Clemente-Juan, C. Mackiewicz, M. Verelst, F. Dahan, A. Bousseksou, Y. Sanakis, J.-P. Tuchagues, *Inorg. Chem.* **2002**, *41*, 1478.

[16] "*MINUIT Program*, a System for Function Minimization and Analysis of the Parameters Errors and Correlations": F. James, M. Roos, *Comput. Phys. Commun.* **1975**, *10*, 345.

[17] a) J. J. Borrás-Almenar, J. M. Clemente-Juan, E. Coronado, B. S. Tsukerblat, *Inorg. Chem.* **1999**, *38*, 6081; b) J. J. Borrás-Almenar, J. M. Clemente-Juan, E. Coronado, B. S. Tsukerblat, *J. Comput. Chem.* **2001**, *22*, 985.

Received: April 18, 2008
Published Online: July 14, 2008

